Chapter 18
Peculiarities of Liquid Crystal—Carbon Nanotube Dispersions Doped with a Minute Amount of Nanoparticles of Synthetic Clay

S. Tomylko, O. Yaroshchuk, O. Kovalchuk and N. Lebovka

Abstract It is shown that adding of a small amount (0.1 wt %) of organomodified laponite (LapO) nanoplatelets results in drastic changes in dielectric and electro-optical characteristics of the suspensions of carbon nanotubes (CNTs) in nematic liquid crystal E7. The addition of LapO leads to the absence of classical percolation of conductivity and dielectric constant, as well as reduction of Frederiks threshold and significant growth of contrast ratio of the E7-CNTs samples.

18.1 Introduction

Among the many nanoparticles used as fillers of liquid crystals (LC), carbon nanotubes (CNTs) are of particular interest. These particles, which can be considered as rolled graphene nanolayers are characterized by enormous value of length to diameter ratio (aspect ratio), which can be as high as several thousands. They exhibit extraordinary mechanical strength, highly anisotropic electrical and thermal properties.

Because of high aspect ratio and strong interaction with LC molecules ($E_{LC\text{-}CNT} \sim 2$ eV), CNTs well integrate in LC [1–3]. They bring new properties to LC hosts and allow one drastically reducing the intrinsic drawbacks of these materials that appear when using them in displays and other electro-optic devices.

S. Tomylko (✉) · O. Yaroshchuk · O. Kovalchuk
Institute of Physics, NASU, Prospekt Nauky 46, 03028 Kyiv, Ukraine
e-mail: tomulkosv@ukr.net

O. Kovalchuk
Kyiv National University of Technologies and Design, Nemirovich-Danchenko St. 2, 01011 Kyiv, Ukraine

N. Lebovka
Institute of Biocolloidal Chemistry, NASU, Vernads'koho Boulevard 42, 03142 Kyiv, Ukraine

O. Fesenko et al. (eds.), *Nanomaterials Imaging Techniques, Surface Studies, and Applications*, Springer Proceedings in Physics 146,
DOI: 10.1007/978-1-4614-7675-7_18,

Furthermore, introduction of CNTs may result in untypical responses of LC layers such as effect of electro-optical memory in the nematic [3–5] and isotropic [6] phase. On the other hand, LC is a unique host for CNTs allowing ones to obtain orientationally ordered ensembles of CNTs with readily controllable ordering axis.

The properties of LC-CNT composites strongly depend on structural organization of nanotubes. It is well known that CNTs tend to aggregate forming developed aggregates and even continuous network at higher concentration. Efficiency of this process can be affected by many factors. The most known of them is surface modification of CNT. In this study, we extend to the LC-CNT suspensions a more peculiar approach, known for more than a decade for dispersions [7]. This approach is that the particles of other sort and properties are brought in a studied composite.

As the additional particles we use the nanoplatelets of clay, which are proven to have high affinity to CNTs and well exfoliate in LCs. As those, we earlier utilized organically modified particles of natural clays (Montmorillonite (MMT)) [8]. However, the results appeared quite ambiguous and highly dependent on origin of clay minerals. In the present research, we apply a synthetic clay Laponite (Lap) mainly because of two reasons. First, the synthetic particles have identical chemical content and structure, which are well controlled in the course of synthesis. Second, the size of Lap platelets is much smaller than the size of MMT platelets ($\sim$10 nm versus $\sim$10 μm), so they naturally belong to the category of nanoparticles. We demonstrate that addition of small amount of Lap cardinally changes dielectric and electro-optic properties of LC-CNT composites opening new horizons for application of these composites.

18.2 Experimental Section

18.2.1 Materials

We used a nematic LC E7 from Merck, which is the eutectic mixture of three cyanobiphenyl and one cyanotriphenyl compound. The temperature of its nematic-to-isotropic transition is 58 °C. At room temperature, the dielectric constants of this mixture in the directions parallel and perpendicular to the LC director are $\varepsilon_{/\!/} = 19$ and $\varepsilon_{\perp} = 5.2$, respectively. As CNTs, we utilized the multi-walled carbon nanotubes from Spetsmash Ltd. (Kyiv, Ukraine), produced from ethylene by the chemical vapor deposition method [9]. These CNTs had an outer diameter 20–40 nm, and the length 5-10 μm. The specific electric conductivity σ of the powder of the compressed CNTs was about 10 S/cm.

The clay was Laponite from Rockwood Additives Ltd., UK Its formula is $Na_{0.7}$ $[(Si_8Mg_{5.5}Li_{0.4})\ O_{20}\ (OH)_4]$. It is a powder, in which the disc-like nanoplates of the clay are packed into stacks. The thickness and diameter of these discs are about 1 nm and 25–30 nm, respectively. The faces of disks have a constant negative

charge, while the surface charge of their edges is pH-dependent and positive in acidic medium [10]. As described elsewhere [11], the platelets of original Laponite were modified by ion-exchange reactions with the surfactant cetyltrimethylammonium bromide (CTAB, $C_{16}H_{33}$-$N(CH_3)_3Br$, Fluka, Germany) with 99.5 % purity. The resultant material will be further called as the organomodified Laponite (LapO).

18.2.2 Samples

LCs filled by multi-walled CNTs, LapO, or their hybrid mixtures, were obtained by adding appropriate weights of the CNTs (c = 0.025–0.5 wt %) and LapO (0.1 wt %) to E7 at T = 60 °C with subsequent 10 min sonication of the mixture using an ultrasonic disperser at the frequency of 22 kHz. Then suspensions were kept at room temperature for 24 h, sonicated for 2 min and then loaded by capillary forces into the cells.

The cells for electro-optical and dielectric measurements were made from glass substrates, containing patterned ITO electrodes and aligning layers of polyimide AL3046 (JSR, Japan) for planar alignment. The polyimide layers were obtained by spin coating technique backed at 180 °C for 90 min and rubbed by a fleecy cloth in order to provide a uniform planar alignment of LC in the field-off state. The cells were assembled so that the rubbing directions of the opposite aligning layers were antiparallel or perpendicular, thus the antiparallel or twisted cells were obtained. The antiparallel cells were further used in dielectric studies, while the twisted cells were used for electro-optic measurements. The cell gap d was maintained by 20 μm glass spacers.

18.2.3 Methods

The dielectric studies were conducted by oscilloscopic method [12]. The experimentally measured values of the resistance R and capacitance C of the LC cells were used for calculation of dielectric constants ε' and ε'', respectively. The constants ε' and ε'' were determined in a wide frequency range, $f = 10^{-1}-10^{6}$ Hz, allowing one to plot dielectric spectra of the samples. The value of ε'' was further used for calculation of the sample conductivity σ from the formula $\sigma = 2\pi\varepsilon_0 \varepsilon'' f$. Furthermore, the Cole–Cole diagrams $\varepsilon''(\varepsilon')$ were plotted to determine the width of the near-electrode dielectric layers λ and the time τ of the near-electrode relaxation [13].

The electro-optical measurements were carried out using setup described in [14]. In these experiments, the transmittance of the twist cells, T, placed between two parallel polarizers, was measured as a function of the applied AC voltage U ($f = 2$ kHz) ramped up from 0 to 30 V. The cells were operated in a waveguide

regime (the Mauguin's regime) [15], so that polarization of the testing light followed the LC director, which experienced rotation in 90°. The electro-optic contrast CR was calculated on the basis of $T(U)$ curve, according to formula $CR = T_s/T_0$, where T_0 and T_s are the transmittance values in the initial and saturated states, respectively. Also, the threshold voltage of electric switching (Frederiks's threshold) was estimated as the voltage corresponding to the transmittance value $T_0 + 0.1(T_s–T_0)$.

18.3 Results and Discussion

18.3.1 Dielectric Properties

The typical dielectric spectra, i.e., frequency dependences of the real ε' and imaginary ε'' parts of dielectric constant ε, are presented in Fig. 18.1 for pure LC, LC-CNT, and LC-CNT-LapO samples at 20 °C. The measured frequency range is divided into three areas. The low-frequency area A ($10^{-1} < f < 10$ Hz for pure LC) corresponds to first relaxation process, attributed to surface dipole polarization and space-charge polarization, which essentially changes the near-electrode concentration of free ions [13]. The moderate frequency area B ($10 < f < 10^4$ Hz for pure LC) reflects the processes of polarization and conduction in the bulk of the sample. In this area, there are no relaxation processes, thus the dielectric constant ε' and conductivity σ are independent of the frequency. The high-frequency area C ($10^4 < f < 10^6$ Hz for pure LC) is associated with another relaxation processes—dipole relaxation in the bulk, associated with rotation around the short molecular axis [15]. Further we consistently consider the dielectric properties of composites in the B and A areas of the frequency range.

18.3.1.1 Bulk Dielectric Properties

As it was said above, the permittivity ε' and electrical conductivity σ are frequency independent in B area. The σ (c) curves of LC-CNT and LC-CNT-LapO composites are presented in Fig. 18.2. These data were analyzed using the least-square fitting to the scaling equation

$$\sigma = a\,(c - c_c)^t \tag{18.1}$$

commonly used for characterization of percolation phenomena [16]. In this equation, c_c is the critical concentration of CNTs and t is the conductivity index. Figure 18.2 shows that Eq. (18.1) fits well to the σ (c) curves for LC-CNT series, but the fitting results are unusual compared to the dispersions of CNTs in other matrices. First of all, the critical concentration in all cases is close to 0 ($c_c < 0.02$ wt %). Apparently, this is due to small distance between the electrodes

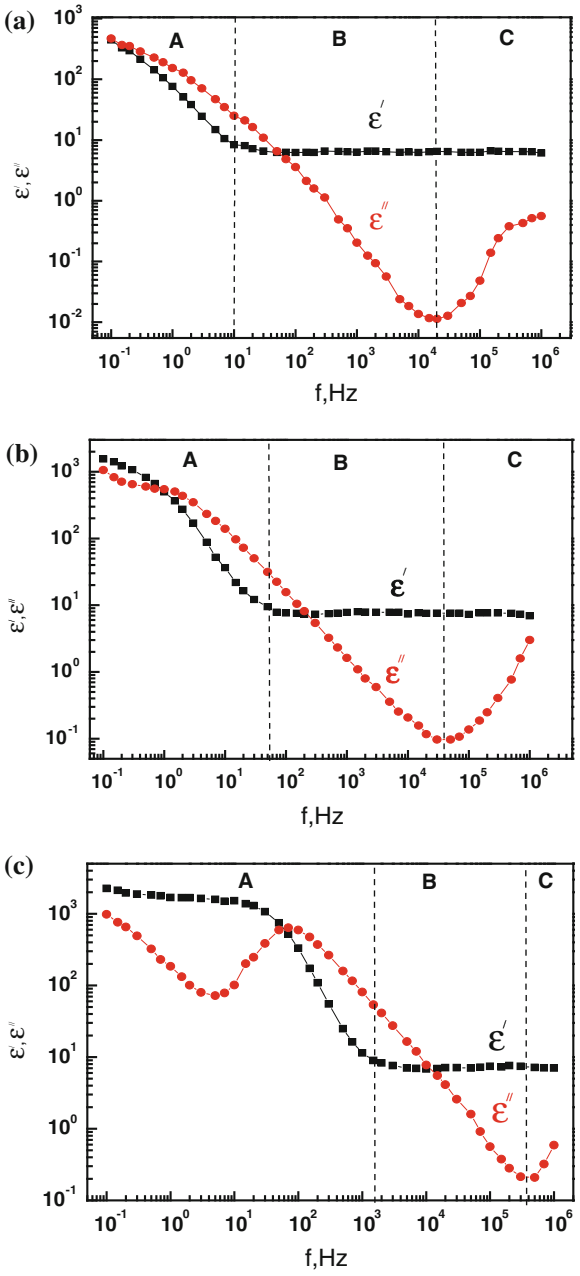

Fig. 18.1 Complex permittivity components ε' and ε'' versus field frequency f for LC E7 **a** E7-CNTs (0.05 wt %) **b** and E7-CNT (0.05 wt %)-LapO (0.1 wt %) **c** samples

($d = 20$ μm), which is comparable to the length of the nanotubes (5–10 μm). This means that the channels of high conductivity, associated with the nanotubes (single nanotubes and their aggregates), start to form in the direction perpendicular to the

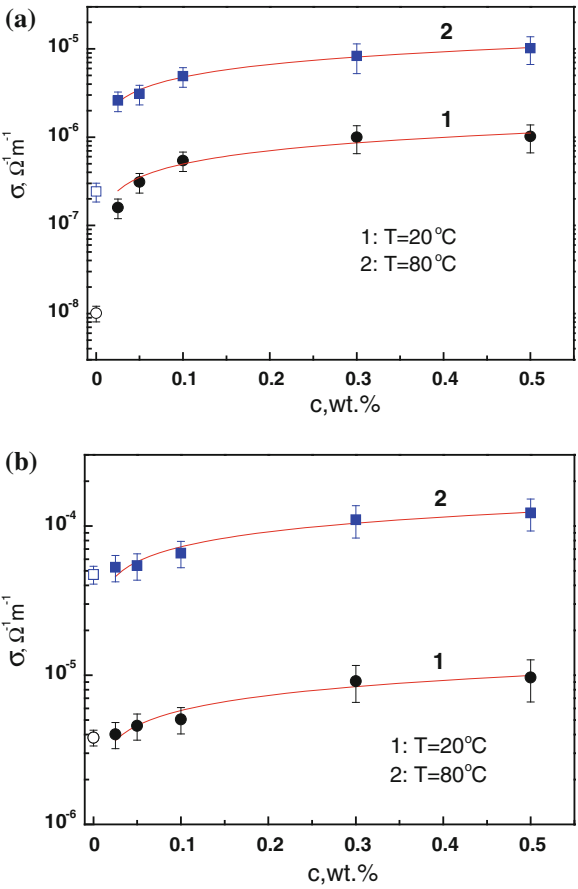

Fig. 18.2 Measured (symbols) and fitted to formula (18.1) (*lines*) conductivity versus CNT concentration *curves* for E7-CNTs **a** and E7-CNT-LapO **b** series. The data corresponding to $c = 0$ (unfilled symbols) are excluded from fitting procedure

composite layer at a very low concentration of CNTs. In contrast to this direction, where the size of aggregates is limited by the cell thickness, in the plane of the composite layer the aggregates can be practically unlimited. In this sense, the aggregates formed in our cells are largely two-dimensional.

The conductivity index t of the samples of LC-CNT series was 0.63 ± 0.08 at 20 °C and 0.48 ± 0.03 at 80 °C. Note that $\sigma(c)$ dependences are essentially sublinear. This indicates that our case is far from the ordinary 3D percolation, characterized by $t \approx 2$ [16]. Indeed, since the length of the nanotubes is comparable to the thickness of the cell, the case of 2D–3D crossover, when the theory predicts the range of $4/3 < t < 2$ [17, 18], suits better for our samples. Nevertheless, even this assumption fails to describe sublinear character of $\sigma(c)$ curves. We believe that such behavior is due to increasing of ion concentration (releasing of the ions from nanoparticles) and solvation of CNTs by LC molecules.

It should be noted that (18.1) describes a $\sigma(c)$ curve for the LC-CNT-LapO series not as good as for the LC-CNT series (there is no clear jump in

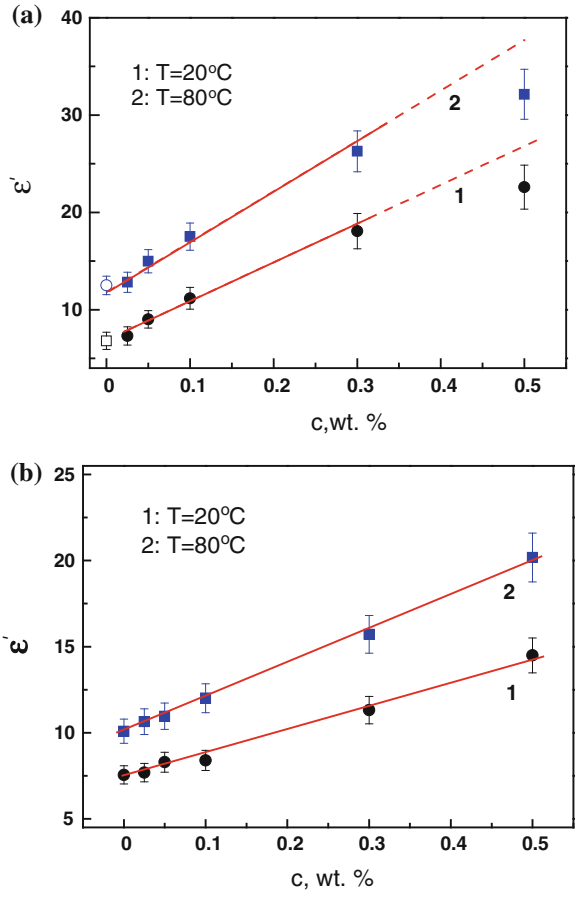

Fig. 18.3 Permittivity versus CNT concentration *curves* for E7-CNTs **a** and E7-CNT-LapO **b** series. The *straight lines* are just for eye guidance

conductivity). However, we use it to compare the $\sigma(c)$ curves for these two series quantitatively. The parameter t for the LC-CNT-LapO series appeared to be two times smaller than for the LC-CNT series: $t = 0.32 \pm 0.04$ (at both 20 and 80 °C). Considerably reduced values of t in the LapO-assisted suspensions give an additional evidence of inhibition of CNT aggregation in an LC. Apparently, the LapO particles, having a great affinity to CNTs, actively surround them. Because of insulation properties of LapO particles, this effect leads to significant reduction in the number of electric contacts between the nanotubes.

The $\varepsilon'(c)$ dependences are shown in Fig. 18.3. It can be seen that ε' monotonically grows with c and increases by about three times with addition of 0.5 wt % of CNTs. The growth of ε' was observed in both nematic and isotropic phases, meaning that it is mainly due to the contribution of the polarizability of nanotubes rather than disturbance of LC orientation by the particles and their aggregates. This result is consistent with the earlier results indicating the increase in LC permittivity with addition of a minute amount of CNTs [19]. The $\varepsilon'(c)$ curve

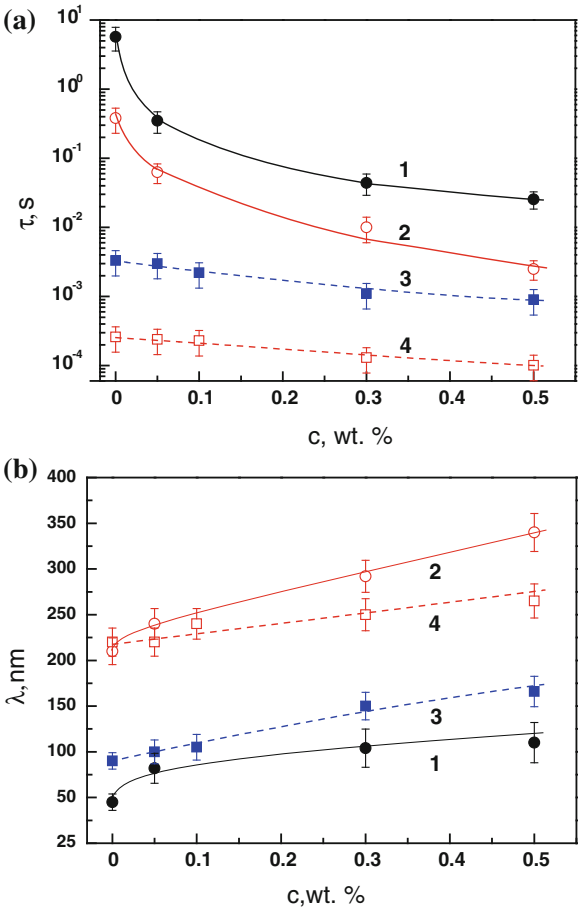

Fig. 18.4 The time of the near-electrode dielectric relaxation **a** and the width of the near-electrode layers **b** as functions of CNT concentration for E7-CNT (curves 1 and 2) and E7-CNT-LapO (curves 3 and 4) series. The curves 1 and 3 correspond to $T = 20$ °C and the curves 2 and 4 correspond to $T = 80$ °C. The *lines* are just for eye guidance

for the LC-CNT series is quasi-linear up to 0.3 wt %. The deviation at higher concentrations c from the linear law can be caused by incomplete filling of CNTs in the cell, since big aggregates are unable to enter the cell. The $\varepsilon'(c)$ curve for the LC-CNT-LapO series is linear over the entire range of CNT concentrations studied in this work. This might reflect improved dispersion of CNTs in the composites containing LapO. The linearity of the $\varepsilon'(c)$ curves suggests that they can be fitted to Maxwell–Wagner mixing equation

$$\varepsilon' = \varepsilon'_{LC} + Kc \tag{18.2}$$

derived in $c \ll 1$ approximation [20]. Here, K is a constant combining permittivity of LC, ε'_{LC}, and CNT, ε'_{CNT}. Thus, despite the fact that our system is above the percolation threshold of conductivity, the Maxwell–Wagner theory still describes effective permittivity. This interesting fact needs further study.

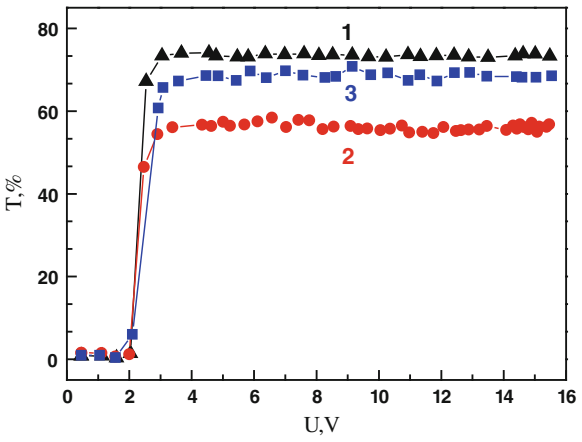

Fig. 18.5 Transmittance versus voltage curves for the E7 *1*, E7-CNT (0.1 wt %) *2* and E7-CNT (0.1 wt %)-LapO (0.1 wt %) *3* samples

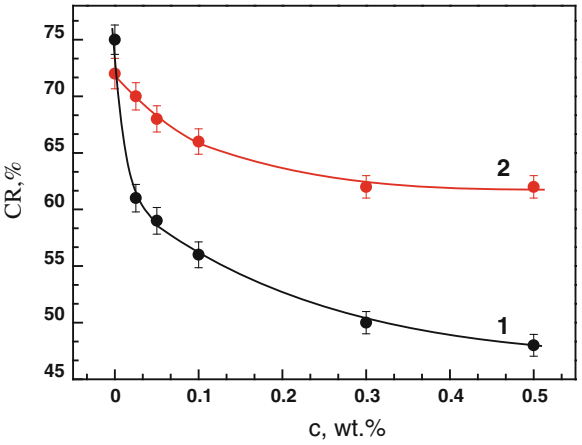

Fig. 18.6 Contrast ratio versus CNT concentration curve for the E7-CNTs *1* and E7-CNTs-LapO *2* series

18.3.1.2 Dielectric Peculiarities in the Near-Electrode Layers

Figure 18.4 presents the effect of addition of CNTs and CNT-LapO particles on the time of dielectric relaxation τ and the width of the near-electrode layers λ of LC cells. In the absence of LapO, the increase in CNT concentration results in a sharp decay of τ at both $T = 20$ and $T = 80$ °C (Fig. 18.4a). Concurrently, a noticeable increase in λ is observed (Fig. 18.4b). A similar tendency was previously described for the LC 5CB doped with CNTs [3]. It was explained by reconfiguration of near-electrode dielectric layers in the presence of CNTs and shunting of these layers by the nanotubes acting as elements of the percolation network. The described effects are weaker in the LapO-assisted LC-CNTs suspensions. For these samples, the $\tau(c)$ curve decays, while the $\lambda(c)$ curve grows according to the exponential law. As it was said above, this may indicate significant interaction of insulating LapO platelets with CNTs. Apparently, it reduces

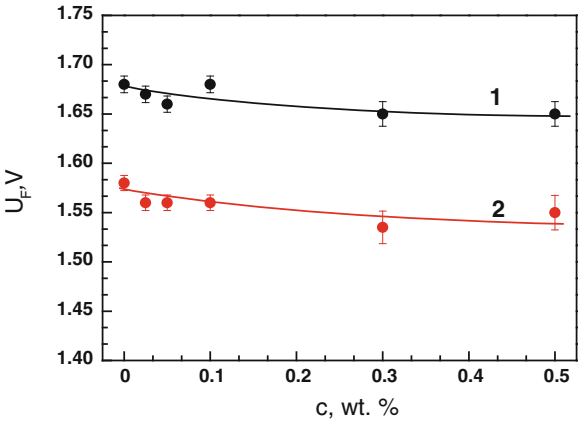

Fig. 18.7 Frederiks threshold voltage versus CNT concentration curves for the E7-CNTs *1* and E7-CNTs-LapO *2* series

efficiency of electrical contacts between the nanotubes and electrodes, as well as between the different nanotubes. It weakens the shunting capability of CNTs and, probably, their interaction with ionic impurities forming the near-electrode layers.

18.3.2 Electro-Optic Properties

The doping by LapO nanoparticles significantly improves electro-optical characteristics of LC-CNT suspensions. The transmittance T versus applied voltage U curves for the twisted cells filled with pure LC E7, E7-CNT (0.1 wt %), and E7-CNT (0.1 wt %)–LapO (0.1 wt %) suspensions are presented in Fig. 18.5. This Figure shows that CNTs mostly affect the saturation value of T. This is mainly due to absorption of testing light by bulky CNT aggregates. However, introduction of a small amount of LapO platelets minimizes this effect, making the $T(U)$ characteristic of LC-CNTs sample close to that of pure LC. Due to improvement of the saturation value of T, the samples containing LapO show higher electro-optic contrast than their LC-CNT counterparts (Fig. 18.6). Finally, we detected inessential decrease in Frederiks's threshold ($\Delta U_F \sim 0.1$ V) in the LapO-assisted LC-CNT suspensions (Fig. 18.7).

18.4 Conclusions

The effect of nanoparticles of organically modified laponite on dielectric and electro-optic properties of the dispersions of multi-walled carbon nanotubes in a nematic LC E7 is investigated. It is found that introduction of a small amount (0.1 wt %) of LapO platelets in an LC-CNT suspension results in essential changes in dielectric properties. In particular, the introduced LapO particles

considerably suppress the percolation character of conductivity and extend the range of linearity of the permittivity versus CNT concentration curve. Furthermore, addition of LapO particles weakens the effect of CNTs on the parameters of the near-electrode layers: changes in the time of dielectric relaxation and thickness of the near-electrode layers become more gradual and thus more controllable with increase in CNT concentration. Finally, the LapO-assisted LC-CNTs dispersions demonstrate considerably improved electro-optic characteristics, such as better switching contrast and reduced threshold voltage. Thus, the proposed approach is rather effective for optimization and diversification of the properties of LC dispersions of CNTs.

References

1. Qi H, Hegmann T (2008) Impact of nanoscale particles and carbon nanotubes on current and future generation of liquid crystal displays. J Mat Chem 18:3288–3294
2. Lagerwall J, Scalia G (2008) Carbon nanotubes in liquid crystals. J Mat Chem 18:2890–2898
3. Dolgov L, Kovalchuk O, Lebovka N, Tomylko S, Yaroshchuk O (2010) Liquid crystal dispersions of carbon nanotubes: dielectric, electro-optical and structural peculiarities. In: Marulanda JM (ed) Carbon Nanotubes, INTECH, Croatia, pp 451–484
4. Dolgov L, Lebovka N, Yaroshchuk O (2009) Effect of electro-optic memory in suspensions of carbon nanotubes in liquid crystal. Colloid J 71(5):603–611
5. Dolgov L, Yaroshchuk O, Tomylko S, Lebovka N (2012) Electro-optical memory of liquid crystal doped by multi-walled carbon nanotubes. Cond Matter Phys 15(3):33401
6. Basu R, Iannacchione GS (2009) Dielectric hysteresis, relaxation dynamics, and nonvolatile memory effect in carbon nanotube dispersed liquid crystal. J Appl Phys 106:124312
7. Tohver V, Smay JE, Braem A, Braun PV, Lewis JA (2001) Nanoparticle halos: a new colloidal stabilization mechanism. PNAS 98(16):8950–8954
8. Lebovka N, Goncharuk A, Bezrodna T, Chashechnikova I, Nesprava V (2012) Microstructure and electrical conductivity of hybrid liquid crystalline composites including 5CB, carbon nanotubes and clay platelets. Liq Cryst 39(5):531–538
9. Melezhyk AV, Sementsov YuI, Yanchenko YV (2005) Synthesis of porous carbon nanofibers on catalysts fabricated by the mechanochemical method. Rus J Appl Chem 78(6):924–930
10. Lysenkov EA, Lebovka NI, Yakovlev YV, Klepko VV, Pivovarova NS (2012) Percolation behaviour of polypropylene glycol filled with multiwalled carbon nanotubes and laponite. Compos Sci Technol 72:1191–1195
11. Zebrowski J, Prasad V, Zhang W, Walker LM, Weitz DA (2003) Shake-gels: shear-induced gelation of laponite–PEO mixtures. Colloids and Surfaces A: Physicochem Eng Aspects 213:189–197
12. Twarowski AJ, Albrecht AC (1979) Depletion layer studies in organic films: low frequency capacitance measurements in polycrystalline tetracene. J Chem Phys 20(5):2255–2261
13. Sawada A, Tarumi K, Naemura S (1999) Effects of electric double layer and space charge polarization by plural kinds of ions on complex dielectric constant of liquid crystal materials. Jpn J Appl Phys 38(3A):1418–1422
14. Zakrevska S, Zakrevskyy Y, Nych A, Yaroshchuk O, Maschke U (2002) Electro-optics of liquid crystal-aerosil-photopolymer composites. Mol Cryst Liq Cryst 375:467–480
15. Blinov L (2011) Structure and properties of liquid crystals. Springer, Dordrecht
16. Stauffer D, Aharony A (1994) Introduction to percolation theory. (2nd ed.) CRC Press, USA
17. Lebovka NI, Manna SS, Tarafdar S, Teslenko N (2002) Percolation in models of thin film depositions. Phys Rev E 66:66134

18. Müller K-H, Wei G, Raguse B, Myers J (2003) Three-dimensional percolation effect on electrical conductivity in films of metal nanoparticles linked by organic molecules. Phys Rev B 68:155407
19. Basu R, Iannacchione GS (2010) Orientational coupling enhancement in a carbon nanotube dispersed liquid crystal. Phys Rev E 81:051705
20. Choy TC (1999) Effective medium theory. Oxford Clarendon Press, New York